

Multiscale Materials in Topology Optimized Vehicle Design

Dr. Richard Beblo
2790 D Street, B20065
Wright-Patterson AFB, OH 45433
USA

Richard.Beblo.1@us.af.mil

ABSTRACT

The next generation of aircraft require novel designs capable of enduring extreme multiphysics environments. Multiscale material Topology Optimization (TO)—where material properties and topology are either simultaneously or sequentially optimized—provides a compelling framework for addressing this complex design problem. In the proposed scheme, a macroscale multidisciplinary topology optimization is constrained with material design constraints derived from a mesoscale material design space exploration. Although this sequential approach provides greater design flexibility, a key drawback is significant computational expense due to the curse of dimensionality. To partially mitigate this expense, we utilize principal component analysis to reduce the order of the radial basis function constraints and a novel sensitivity weighted material design selection approach. The benefit of a sequential scheme is the framework is easily extendable to other disciplines and is material and system agnostic, simplifying collaboration across fields. Results from an optimized Messerschmitt-Bölkow-Blohm (MBB) beam are used to validate the framework, which is then used to design a cylindrical material system attaching two materials with high and low thermal expansion coefficients, approximating the attachment of a compact thermal protection system of a high-speed vehicle, high temperature internal engine components, or a vehicle body panel near a heat source. Experimental results are shown for both the MBB beam and thermal protection system (TPS) cylinder, including digital image correlation and thermal imaging.

RESUME

La prochaine génération d'avions nécessite de designs inédits, capables de supporter des environnements multiphysiques. L'optimisation de la topologie matérielle à plusieurs échelles (en anglais : « Multiscale material topology optimisation », TO) – où les propriétés et topologies des matériels sont optimisés, en simultanée ou en séquence – offre un cadre contraignant qui permet d'adresser cette complexe problématique de design. Dans le schéma proposé dans l'article, nous contraignons une TO multidisciplinaire à l'échelle macro, avec des contraintes de design de matériels basés sur un espace d'exploration à l'échelle méso. Cette approche séquentielle offre plus de flexibilité de design; cependant, un inconvénient majeur sont les dépenses computationnelles dues à la dimensionnalité. Pour atténuer en partie ces dépenses, nous utilisons une analyse en composante principale, afin de réduire les contraintes de la fonction de la base radiale; et une nouvelle approche à la sélection du design du matériel, pondérée en base à la sensibilité. L'avantage d'une approche séquentiel est que le cadre peut facilement s'étendre à d'autres disciplines, proposant une solution souple qui ne dépend ni des matériels, ni du système, et qui par conséquent simplifie la collaboration entre différentes spécialités. Les résultats d'un rayon Messerschmitt-Bölkow-Blohm (MBB) optimisé sont utilisées pour valider le cadre, qui est ensuite utilisé pour concevoir un système matériel cylindrique, liant deux matériels aux coefficients d'expansion thermiques élevé et faible, s'approchant ainsi à la jonction du système compact de protection thermique d'un véhicule à haute vitesse, aux composants internes de moteur à haute température, ou au panneau d'un véhicule près d'une source de chaleur. Les résultats expérimentaux pour le rayon MMB et le cylindre du système de protection thermique (en anglais : « thermal protection system », TPS) sont publiés, y inclus la corrélation d'images numériques et les images thermiques.

KEY WORDS

Component analysis; Material design; Multiscale material topology optimization

MILITARY RELEVANCE

In this new era of great power competition and realigning Department of Defense assets and priorities to better equip and ready the force for potential future conflicts, it is imperative that the scientific community develop and transition technologies that close the gaps identified by United States Secretary of the Air Force Frank Kendall's Operational Imperatives (OIs). In particular, the tactical air dominance imperative, and to a lesser extent the global strike imperative, call for a mix of aircraft in size, manning, capability, and cost. One of the key lessons learned from the conflict in Ukraine, and key to the successful realization of the OIs, is the quick and seamless adaptation and implementation of new technology via short design cycles. In 2001, retired Air Force Colonel Mark Gunzinger published a detailed report describing how a large number of low cost systems supported by a relatively few more capable systems may provide a tactical advantage over a peer adversary, a concept known as affordable mass. As the Air Force continues to develop Collaborative Combat Aircraft, providing affordable mass to the suite of platforms needed for future tactical air dominance and global strike, the need to rapidly integrate evolving technologies into these platforms and increase their effectiveness necessitates novel design frameworks. One such capability is simultaneous material and system level design, such as the method detailed in this work, providing the ability to quickly incorporate new materials and sub-systems into a new or updated platform. Being first to the fight with a new technology or quickly developing a countermeasure to an adversary's technology can provide considerable tactical advantages.

1.0 DESIGN FRAMEWORK

In multiscale Topology Optimization (TO), the material and structure are designed at both the macroscale and the mesoscale. Multiscale TO allows each discretized element in the macroscale structure to have a custom-designed material or mesostructure, allowing greater design flexibility [1]. Two forms of multiscale TO are concurrent and sequential. Concurrent multiscale TO focuses on inserting a homogenized stiffness matrix directly into the macroscale optimization, effectively optimizing both the macroscale structure and mesoscale unit cell topology, simultaneously. Generally, a maximum of two physical models are considered during concurrent TO, which maintains computational efficiency but limits the utility of such processes in the context of aerospace applications in complex multiphysics loading environments and is often difficult to incorporate new or novel materials or physics. In contrast, sequential multiscale TO frameworks perform the macroscale optimization and mesoscale optimization consecutively. The multiscale TO framework presented here is a sequential scheme in which models that bound potential mesoscale responses are defined first and then passed directly to the macroscale optimizer [2], [3]. Once the macroscale optimization is complete, the mesoscale topologies that match these homogenized responses can be determined.

It should be noted the material system used in the presented work to demonstrate the utility of the framework is a Parametric Lindenmayer system, or L-system, material [6]. Materials are grown organically using a system of rules and parameters (Figure 1, left). An interpreter then creates a truss-like component, resulting in a hierarchical material structure utilizing the row of characters as instructions and a given graph (design volume), such as a square or cube (Figure 1, center). The resulting material topologies (Figure 1, right) are then analyzed and their properties homogenized. These homogenized properties are then described by radial basis functions (RBF). It is important to note there is no reverse mapping of an L-system material. Meaning there is no equation that can be derived from a known geometry that results in a unique set of instructions. Nor is there a closed form equation describing the resulting material properties from a set of instructions. This lack of a system model necessitates the presented framework approach.

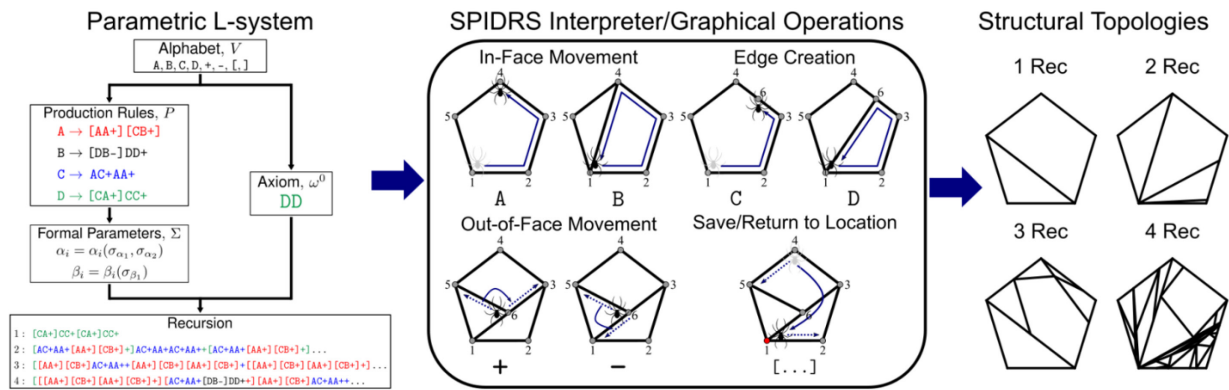


Figure 1: Lindenmayer system material description.

An overview of the multiscale TO framework, described in detail in references [2] and [3], is depicted in Figure 2. Step one involves exploring the design space of the material using a non-dominated sorting genetic algorithm, NSGA-II, resulting in a point cloud of material designs. Although we are using a genetic algorithm (GA), the design space could be populated by interrogating a material model, subsystem model, or with experimental data. Homogenized material properties of each material design are then determined via finite element analysis. The boundaries of the design space are identified (i.e., the limits of the capabilities of the material system), which are then fit with RBF. One could simply set the order or degree of the RBF equal to the number of design variables to fully capture all variability, but this quickly becomes intractable with large numbers of design variables. To limit the complexity of the RBFs, one can employ partial correlation coefficients describing the degree of variability in the data with respect to each design variable and eliminate unnecessary material parameters. Thus, only material properties with sufficient influence over the objective function are included in the radial basis function fit of the boundaries of the design space. A more rigorous treatment, however, is utilizing principal component analysis. Rather than the RBF coefficients being determined by the material properties (i.e., design variables) themselves, the data is transformed using eigen analysis, resulting in each RBF coefficient containing data relating all design variables simultaneously. The order of the RBF is then entirely a function of the degree to which the user desires to describe the variability in the data, similar to approximating a trigonometric function with the first few terms of a Fourier series expansion. The result is a set of RBF functions collectively encasing a closed design space.

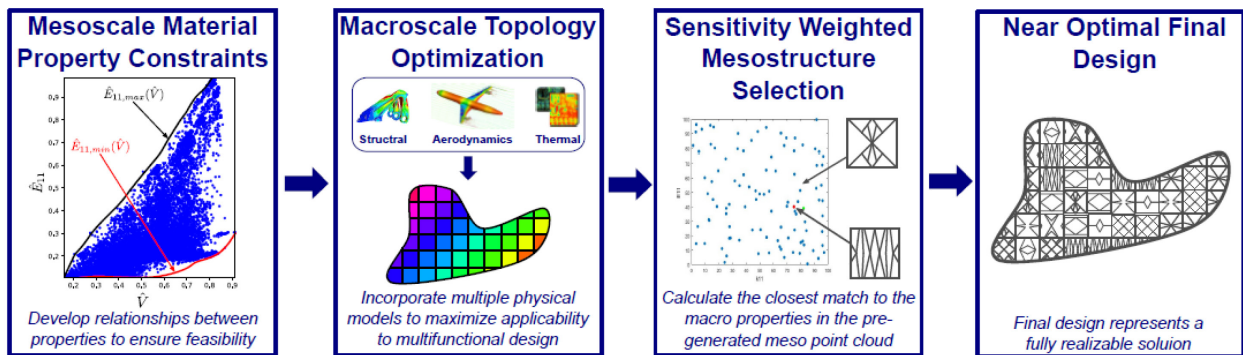


Figure 2: Multiscale TO framework functional diagram [2], [3].

In step two, these functions are used as constraints in a gradient-based multidisciplinary topology optimization using a Method of Moving Asymptotes (MMA) algorithm, where the objective function is a combination of thermal resistivity and structural compliance and the cost function is either weight or volume. The RBF material

constraints ensure that a resulting set of material properties remain within a physically realizable limit. Unique material properties are determined, optimizing the system level performance of the design for each voxel, or design volume. Typical material properties include Young's moduli, shear moduli, Poisson's ratio, thermal conductivity, thermal expansion coefficients, and damping ratios in each of the three cardinal directions.

In step three, two options are available: 1) materials specific to the desired requirements of each voxel are designed; or 2) material designs with similar properties to the desired set are chosen from the set of material designs generated in step 1 [4], [5]. This can be accomplished using either simple Euclidean distances between design points or, more optimally, using a sensitivity weighted function. The objective function is differentiated with respect to each design variable and the resulting sensitivities determined for each voxel (Equation 1). The sensitivities are then normalized in Equation 2. The material design resulting in the least change to the objective function is then found by minimizing the set of distances (Equation 3) between the desired set of material properties and the available materials from step one in Figure 2. It should be noted the performance difference between the ideal structure and the closest to ideal using the above sensitivity weighted method of choosing already available materials is entirely dependent upon the density of available materials within the design space.

$$S_1 = \frac{\partial C}{\partial E_{11}}, S_2 = \frac{\partial C}{\partial \nu_{12}}, S_3 = \frac{\partial R}{\partial k_{11}}, \dots \quad (1)$$

$$\hat{S}_1 = S_1 / (S_1 + S_2 + S_3 + S_4 + S_5 + S_6 + \dots) \quad (2)$$

$$D_{SW} = \left[\hat{S}_1^2 (E_{11} - E_{11pc})^2 + \hat{S}_2^2 (\nu_{12} - \nu_{12pc})^2 + \hat{S}_3^2 (k_{11} - k_{11pc})^2 + \hat{S}_4^2 (G_{12} - G_{12pc})^2 + \dots \right]^{1/2} \quad (3)$$

Finally, in step four, the realizable material parameters are assigned to their respective voxels and a final system level performance analysis is completed.

2.0 FRAMEWORK VALIDATION

2.1 MBB Beam

The above framework was utilized to design a minimal weight MBB beam, shown in Figure 3, with a heat source along the top and a sink along the side. Upon careful inspection of the design, one can easily see voxel designs with high stiffness in the horizontal direction along the top and bottom surfaces and voxels with high shear stiffness near the center. One can also see voxels with high horizontal thermal conductivity near the right edge as expected. A more complete analysis of the results and optimality of the design can be found here [7], which includes an experimental structural validation of the finite element analysis (FEA) results using a 3-point bend test and 3D printed polymer test article.

2.2 Thermal Cylinder

To further validate and demonstrate the utility of the method, the framework was used to design a material to structurally attach a solid inner cylinder to a carbon-carbon composite outer cylinder. The inner cylinder approximates a low temperature load bearing structure with high thermal expansion and the outer cylinder approximates a high temperature, low thermal expansion thermal protection system (TPS). A constant temperature was applied to the exterior of the cylindrical design space and a static load applied to the inner ring. The resulting design and test article are shown in Figure 4, consisting of two concentric rings of voxel designs designed to accommodate differing amounts of strain across a wide temperature range, while maintaining structural integrity.

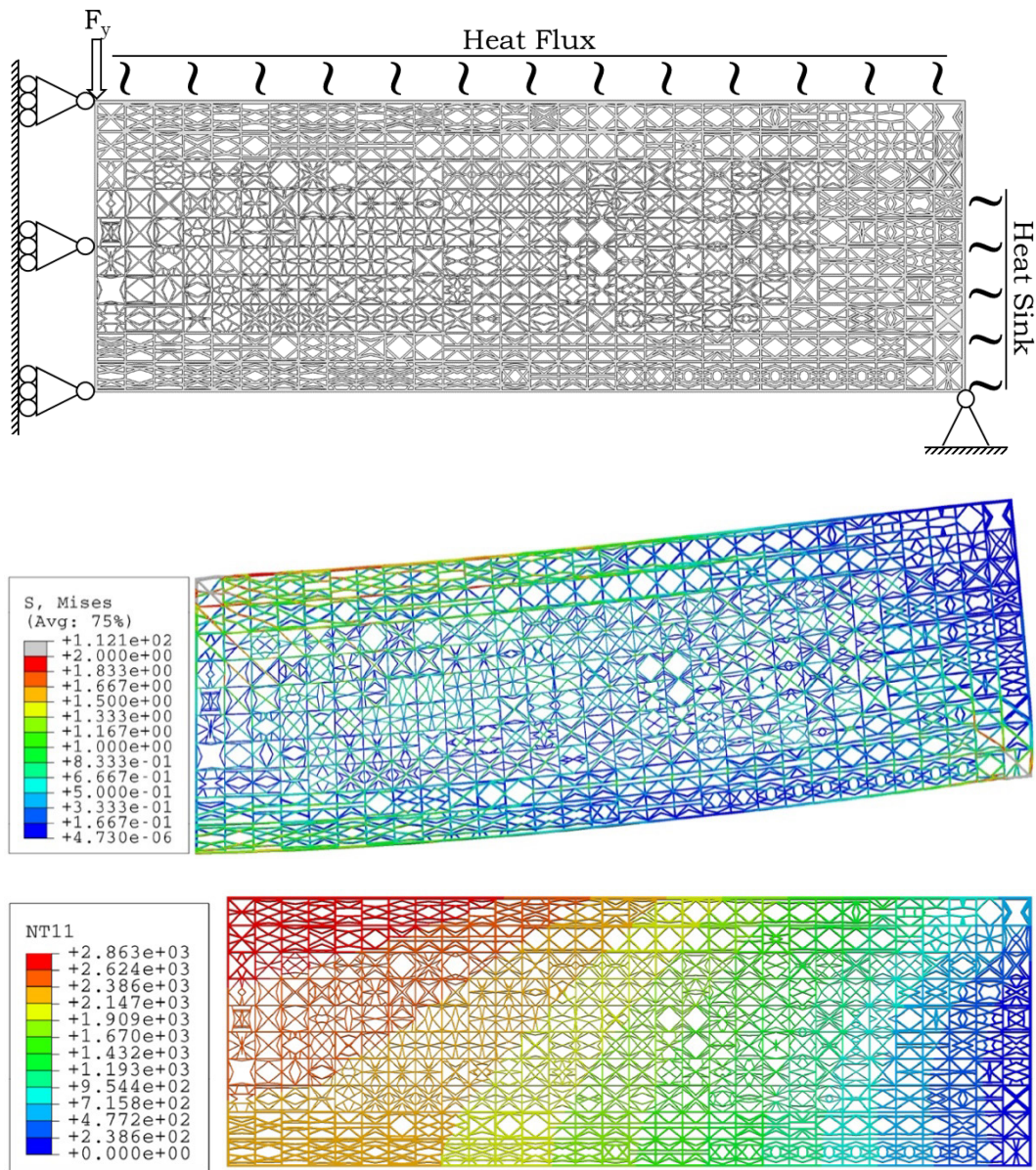


Figure 3: MBB Beam design and boundary conditions (top), Von-Mises stress (MPa) (middle), and steady state temperature (Kelvin) (bottom).

The test article was 3D-printed in Inconel 718 using a Laser Powder Bed Fusion (LPBF) process, which required the addition of internal supports. The individual slender members within the test article are approximately 0.5 mm in diameter. The test article was suspended using Alumina-bisque ceramic rods and heated using four Hi-TempIR 5203-10 infrared heaters arranged 90 degrees in a circumference around the test article (Figure 5, right). Digital Image Correlation (DIC) was performed with two FLIR BFS-U3-88S6M-C cameras with Edmund Optics 35mm lenses, linear polarizing filters to reduce glare, and Edmund Optics 500 nm bandpass filters. Two Larson Electronics 25W Blue LED spotlights illuminated the test article and an Optris PI 640i thermal camera provided full field temperature measurements. The test article was also instrumented with several Extrinsic Faby-Perot Interferometer (EFPI) and WK strain gauges and K-type thermocouples, Figure 5.

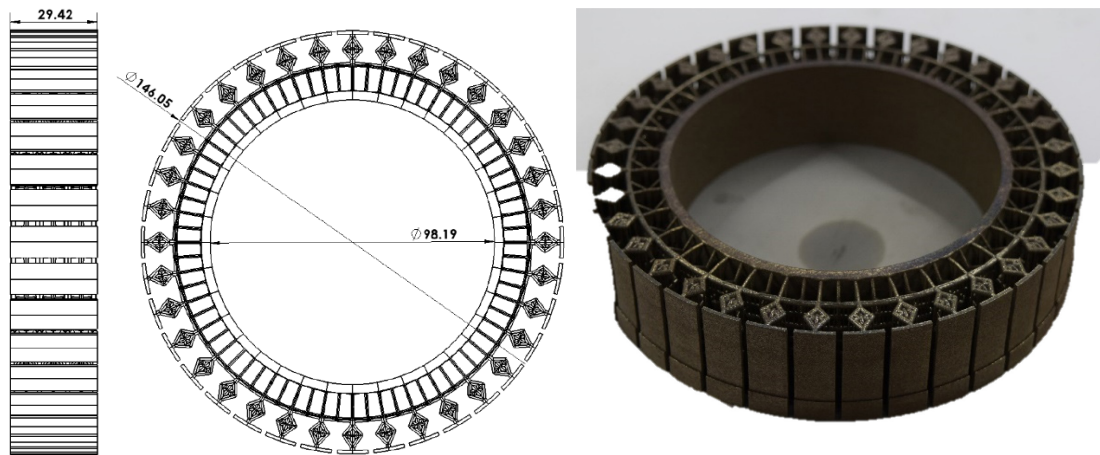


Figure 4: Test article design (left) and 3D printed test article (right). The carbon-carbon outer ring is not shown (dimensions in mm).

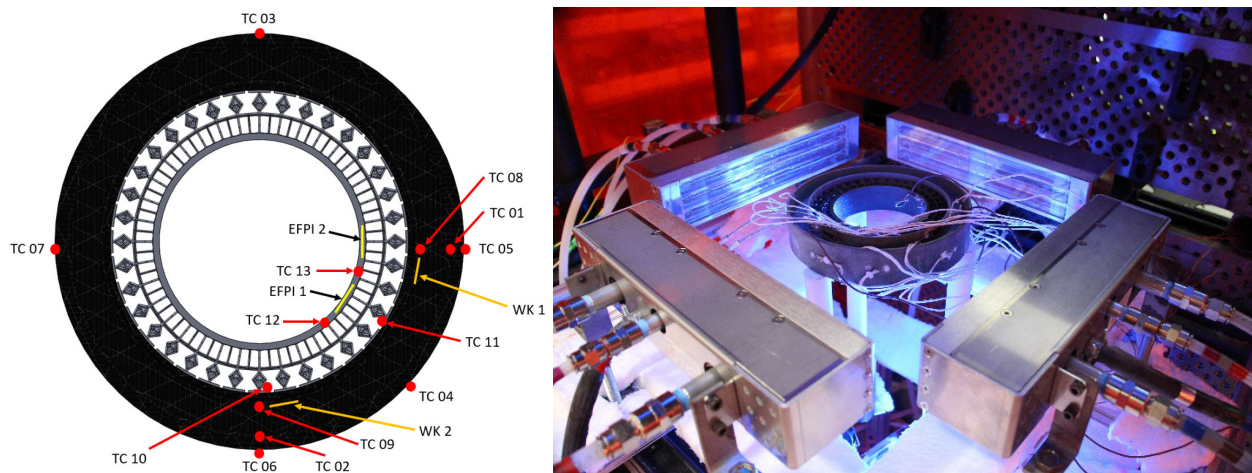


Figure 5: Test article strain and temperature gauge instrumentation (left) and experimental setup (right).

For the test shown in Figure 6 to Figure 8, the outside surface temperature of the carbon-carbon ring was raised to 500F and held constant for 1000s by cycling the heaters on and off via a control system. The system approaches steady state after about 800 seconds with a desired typical temperature gradient across the test article, Figure 6 and Figure 7. The FEA solution shows excellent agreement with Infrared (IR) and thermocouple data.

As shown in Figure 6 Right and Figure 8, the circumferential strain within the carbon-carbon ring near the interface with the Inconel test article (WK1) is significantly lower than that of the solid Inconel inner cylinder (EFPI1). This is expected due to the carbon-carbon composite's extremely low thermal expansion coefficient. As indicated by DIC results (Figure 8 Left) and FEA analysis (Figure 8, Right), the majority of this strain mismatch is accommodated by the designed structural members between the solid inner and outer cylinders.

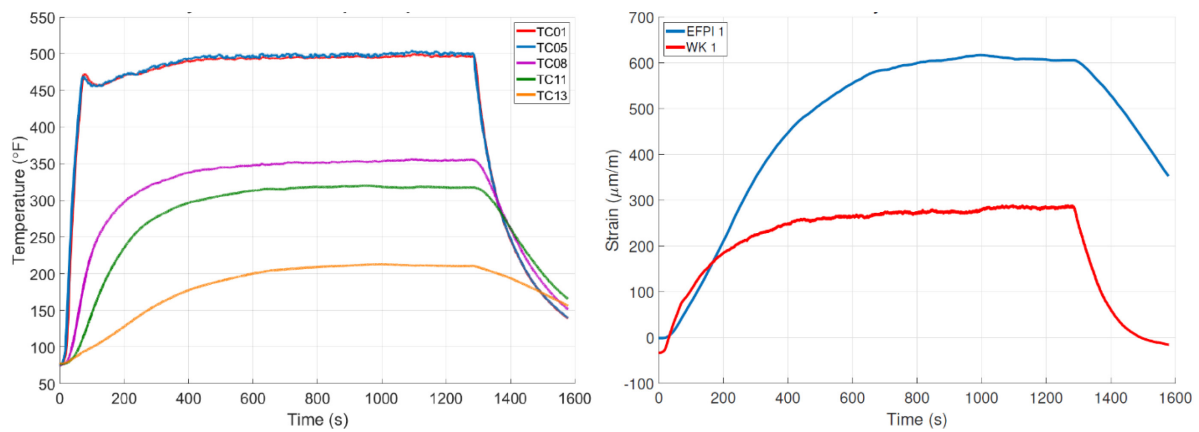


Figure 6: Experimental temperature profiles of several thermocouples (left) and circumferential strain near the solid inner cylinder (EFPI1) and at the interface between the Inconel and carbon-carbon ring (WK1) (right).

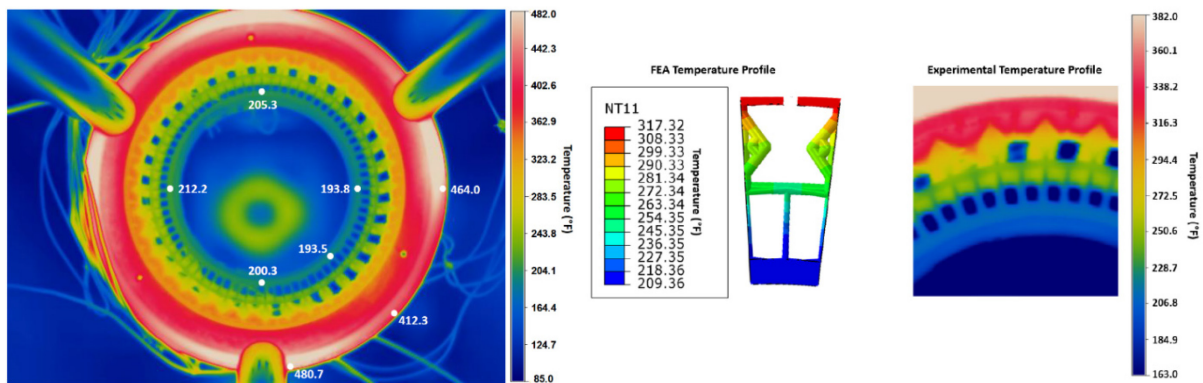


Figure 7: Full field experimentally measured IR temperature at about 800s (left) and zoomed in area of interest (right) compared to the analytically calculated temperature profile using FEA (center) temperatures showing good agreement across the test article.

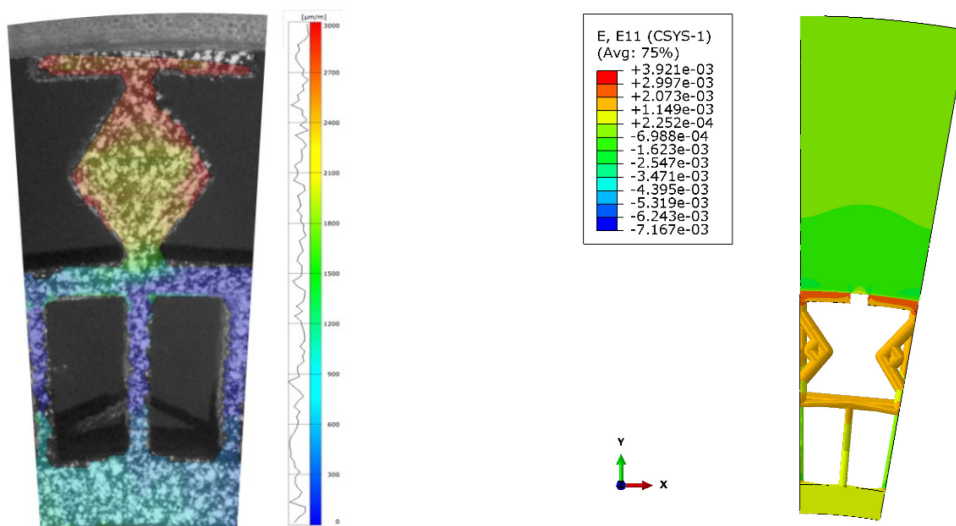


Figure 8: Experimental circumferential DIC strain profile (left) compared to FEA (right). The experimental data ranges from 0 to 3000 micro strain.

3.0 CONCLUSIONS

Although much work remains in validating the framework and extending it to include more physics, multiple materials, more complex design domains, and accommodating more design variables, the above work shows promise in the method as a viable solution to incorporating material design into topology optimization. Principal component analysis has been shown to have the capability of incorporating variation of up to 50 different design variables at relatively low order. The method of using RBFs to model the boundaries of the material design space appears adequate given appropriate smoothing of the functions during fitting. Using homogenized material properties, executing the macroscale optimization yields a relatively computationally efficient process. Using sensitivity weighted nearest neighbor for realizable material selection has minimal detrimental impact on optimality.

4.0 VARIABLES, SYMBOLS, AND ABBREVIATIONS

3D	Three Dimensional
DIC	Digital Image Correlation
DSW	Sensitivity Weighted Distance Between Two Materials
EFPI	Extrinsic Faby-Perot Interferometer (strain gauge)
FEA	Finite Element Analysis
GA	Genetic Algorithm
IR	Infrared
LPBF	Laser Powder Bed Fusion
L-system	Parametric Lindenmayer system
MBB	Messerschmitt-Bölkow-Blohm
MDAO	Multidisciplinary Design, Analysis, and Optimization
MMA	Method of Moving Asymptotes
NSGA	Non-dominated Sorting Genetic Algorithm
RBF	Radial Basis Function
TPS	Thermal Protection System
C	Structural Compliance
E	Young's Modulus
G	Shear Modulus
k	Thermal Conductivity
R	Thermal Resistivity
S	Design Variable Sensitivity
\hat{S}	Normalized Design Variable Sensitivity
Subscripts 1, 2, 3	Cardinal Directions
Subscript pc	Denotes Realizable Material Contained in the Point Cloud
Subscript SW	Denotes a Sensitivity Weighted Property

5.0 REFERENCES

- [1] Sivapuram, R., Dunning, P., and Kim, A., “Simultaneous Material and Structural Optimization by Multiscale Topology Optimization,” *Structural and Multidisciplinary Optimization*, 54(5), 1267-1281, 2016.
- [2] Bielefeldt, B., Beblo, R., Lawson, K., and Lowe, R., “Development of Material Property Feasibility Constraints for a Multiscale Topology Optimization Framework Using Radial Basis Function Interpolations,” *ASME SMASIS 2022*, 2022.
- [3] Bielefeldt, B., Beblo, R., Deaton, J., Lawson, K., and Lowe, R., “Exploring a Multiscale Topology Optimization Design Space Using a Parametric L-system Approach,” *AIAA SciTech 2022 Forum*, 2524, 2022.
- [4] Lawson, K., “Exploration of Data Clustering Within a Novel Multi-Scale Topology Optimization Framework,” *MS Thesis, University of Dayton*, 2022.
- [5] Meixner, E., Lowe, R., Bielefeldt, B., Beblo, R., “Sensitivity-Weighted Mesostructure Selection within a Multiscale Topology Optimization Framework,” *AIAA SciTech Forum*, 8–12 Jan 2024, Orlando, FL, USA.
- [6] Bielefeldt, B. “Multiobjective Topology Optimization for Preliminary Design Using Graph Theory and L-System Languages,” *Texas A&M University, dissertation*, 26 Mar 2020.
- [7] Meixner, E., Lowe, R., Bielefeldt, B., Beblo, R., “Sensitivity-Weighted Mesostructure Selection within a Multiscale Topology Optimization Framework,” *AIAA* (under review).

ACKNOWLEDGEMENTS

This work was supported by the U.S. Air Force Office of Scientific Research under Grant No. 22RQCOR002.

